Food Hydrocolloids 144 (2023) 108973

Contents lists available at ScienceDirect

Food Hydrocolloids

journal homepage: www.elsevier.com/locate/foodhyd

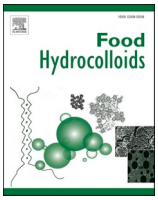

# Thermal hysteresis phenomena in aqueous xanthan gum solutions

Emmanuel M. Nsengiyumva [1,2], Mark P. Heitz [1,*], Paschalis Alexandridis [2,**]

[1] Department of Chemistry and Biochemistry, The State University of New York (SUNY) Brockport, Brockport, NY, 14420, USA
[2] Department of Chemical and Biological Engineering, University at Buffalo, The State University of New York (SUNY), Buffalo, NY, 14260-4200, USA

ARTICLE INFO

*Keywords:*
Biopolymer
Polysaccharide
Xanthan gum
Rheology
Viscosity
Thermal history

ABSTRACT

The anionic hydrocolloid polysaccharide xanthan gum is widely used in the food and petroleum industries (among others) as a viscosity enhancement polymer due to its high viscosity at low concentrations and moderate temperatures. The physical properties of microbial polysaccharide xanthan gum aqueous solutions were investigated using temperature dependent viscosity measurements. Specifically, the effect of thermal history on the solution viscosity was investigated. Heating and cooling cycles were assessed in two ways, by using a "sawtooth" and "triangle" pattern, which essentially differed in the rates of cooling. The sawtooth method used a cooling rate of 2.0 °C $min^{-1}$ whereas the triangle pattern had a cooling rate of 0.20 °C $min^{-1}$. The sawtooth cooling rate was controlled by the speed at which the Peltier device could cool the sample, and the triangle rate was governed by the time required to measure the viscosity at each temperature on return to the initial value. Cycles measured using the sawtooth pattern for 16 mg/kg xanthan gum in water showed an 8–10% overall decrease in the viscosity over four complete cycles. Comparatively, at 320 mg/kg the xanthan gum solution showed a 25% decrease in viscosity over four cycles. The observed temperature dependent viscosity variation suggested minor modifications in the physical network structure of xanthan gum. When using a triangle heating/cooling pattern, the overall decrease in the xanthan gum solution viscosity was 5–7% for 16 mg/kg and only 10% change for 320 mg/kg solutions. The activation energy of viscous flow for the aqueous xanthan gum solutions by either method was ~15.0 kJ/mol under all conditions. The data showed that temperature and heating cycles influence xanthan gum viscosity and thermal history, which depends more strongly on xanthan gum concentration than solution temperature.

## 1. Introduction

Biopolymers abound in nature and derive from renewable resources such as plants, animals, and microorganisms, and includes polysaccharides, proteins, nucleic acid, etc. (Klemm, Heublein, Fink, & Bohn, 2005; Maarel, 2008; Mendonça, Morais, Pires, Chung, & Oliveira, 2020; Xia et al., 2020). Carbohydrate polymer systems find diverse applications, such as pharmaceuticals (Yu, Shen, Song, & Xie, 2018), biomedicals (Petri, 2015), cosmetics, tissue engineering (Kumar, Rao, & Han, 2018), food processing (Brunchi, Morariu, & Bercea, 2021; Wyatt & Liberatore, 2010), and oil and gas extraction (Ahmad et al., 2021; Chatterji & Borchardt, 1981; Wever, Picchioni, & Broekhuis, 2011). Polysaccharides are promising materials because of their function, such as thickening, stabilizing, suspending, or emulsifying agents, and are considered sustainable and environmentally friendly materials (Capron, Brigand, & Muller, 1997; "KELTROL®/KELZAN® xanthan gum. Book 8th edition," 2001–2008). In the polysaccharide family, xanthan gum garners broad interest in many application prospects because of its inherent physicochemical properties. Xanthan gum is an anionic hydrocolloid, an extracellular polysaccharide produced from the fermentation of the *Xanthomonas campestris* bacterium (Margaritis & Zajic, 1978). The ability of xanthan gum to control solution properties (i.e., build a high viscosity at low concentration) has promoted its use as a rheology modifier in various industries (Abu Elella et al., 2021; Ahmad et al., 2021; Wever et al., 2011). The chemical structure of xanthan gum is of prime importance in determining its solution properties.

The primary structure of xanthan gum was established in 1975 and varies based on the side chain substituents present (Jansson, Kenne, & Lindberg, 1975; Melton, Mindt, Rees, & Sanderson, 1976). The chemical structure of xanthan gum, shown in Fig. 1, consists of a $\beta$-1,4-linked glucan backbone with charged trisaccharide side chains ($\beta$-D-manopyrannosyl-(1,4)-$\alpha$-D-glucopyrannosyl-(1,

* Corresponding author.
** Corresponding author.
*E-mail addresses:* mheitz@brockport.edu (M.P. Heitz), palexand@buffalo.edu (P. Alexandridis).

https://doi.org/10.1016/j.foodhyd.2023.108973
Received 28 March 2023; Received in revised form 27 May 2023; Accepted 12 June 2023
Available online 12 June 2023

2)-β-D-mannopyrannosyl-6-O-acetate) on alternating backbone residues (Bercea & Morariu, 2020; Margaritis et al., 1978; Merino-Gonzalez & Kozina, 2017; Morris, 2019; Wyatt et al., 2010). The glucose, mannose, and glucuronic acid units on the polymer backbone have a molar ratio of 2:2:1 (Bhat, Wani, Mir, & Masoodi, 2022; Faria et al., 2011; Miranda et al., 2019), while a molar ratio of 2.8:2.0:2.0 has also been reported (Garcia-Ochoa, Santos, Casas, & Gomez, 2000; Miranda et al., 2019). It is estimated that roughly half of the terminal D-mannose contains a pyruvate group residue that is linked to the keto group at positions 4 and 6, although the distribution of this residue is unknown (Petri, 2015; Sandford & Baird, 1983). Additionally, the D-mannose unit linked to the main chain has an acetyl group at position O-6. The presence of acetic and pyruvic acids renders xanthan gum an anionic polysaccharide (Kool, Gruppen, Sworn, & Schols, 2013, 2014; Orentas, Sloneker, & Jeanes, 1963). Pyruvate (attached to 4,6-cylic acetal) is the conjugate base of pyruvic acid with a three-carbon ketoacid containing carboxylic acid and a ketone group (Abbaszadeh et al., 2015). The pyruvic acid content depends on the fermentation process and the strain of the *Xanthomonas* bacteria (Margaritis et al., 1978). Xanthan gum is a high molecular weight (1-50 $\times$ $10^6$ g/mol (Becker, Katzen, Puhler, & Ielpi, 1998; Garcia-Ochoa et al., 2000; Holzwarth, 1978)) and water-soluble polymer with side chains (glucuronic acid unit and two mannose units) that comprise approximately 65% of the total molecular weight. The multiple hydroxyl and carboxyl groups on the xanthan gum structure contribute to the strong electrostatic repulsions in aqueous media (Krstonošić, Milanović, & Dokić, 2019). Xanthan gum is a fast-hydrated water-soluble hydrocolloid that is easily dissolved in both plain water and salt-containing solutions at room temperature (Capron et al., 1997; Dumitriu, 2005; Viebke, 2005). Depending on the specific environmental conditions, xanthan gum chains may assume either an ordered or disordered conformation (Brunchi, Avadanei, Bercea, & Morariu, 2019; Lopes, Andrade, Milas, & Rinaudo, 1992; Morris & Foster, 1994; Morris, Rees, Young, Walkinshaw, & Darke, 1977; Southwick, Jamieson, & Blackwell, 1982). Upon increasing the ionic strength of the solutions, the hydration tends to be slow, and xanthan gum forms a rigidly ordered conformation at low temperatures. However, the ordered state at low temperature turns to a disordered state, flexible chains with an increase in the temperature, resulting in conformation transition in solution (Nsengiyumva & Alexandridis, 2022).

The secondary structure of xanthan gum exists in three forms: (1) a native, single-stranded helix; (2) a double or triple helix; and (3) a disordered, random coil/flexible chain (Dumitriu, 2005; Milas, Reed, & Printz, 1996; Milas & Rinaudo, 1979; Viebke, 2005). However, structural details of the helical conformation remain controversial (Brunchi et al., 2019; Brunchi, Bercea, Morariu, & Avadanei, 2016; Brunchi, Bercea, Morariu, & Dascalu, 2016; Brunchi, Morariu, & Bercea, 2014). It is observed that the xanthan gum side chains fold and will interact via hydrogen bonding with the gum backbone (Tako, Teruya, Tamaki, & Ohkawa, 2010). Brunchi and coworkers (Brunchi et al., 2019) reported that acetate residue methyl groups bind to hemiacetal oxygens of alternate D-glucose residues. For a disordered conformation, side chains experience electrostatic repulsions that drive separation (Brunchi et al., 2019; Callet, Milas, & Rinaudo, 1987). In addition, studies using light scattering and atomic force microscopy revealed that xanthan gum assumes a double helical structure in aqueous media, associated with chain stiffness, and order-disorder transitions occur with rising temperature (above 50 °C) (Matsuda, Biyajima, & Sato, 2009). The denatured form of xanthan gum, a disordered structure that arises from more flexible chains during temperature treatment, produced higher viscosity than the native state (Brunchi et al., 2019; Brunchi, Bercea, Morariu, & Avadanei, 2016; Brunchi, Bercea, Morariu, & Dascalu, 2016; Brunchi et al., 2014; Rinaudo, Milas, Bresolin, & Ganter, 1999). The native, single helical state of the chains is stabilized by side-chain interactions in aqueous solutions below $10^{-2}$ M salt and at increasing temperatures from 25 to 75 °C (Brunchi et al., 2019; Brunchi, Bercea, Morariu, & Avadanei, 2016; Brunchi, Bercea, Morariu, & Dascalu, 2016; Brunchi et al., 2014). In addition, the denatured state is thought to appear at 80 °C in water. Still, its sensitivity depends on the xanthan gum concentration, molecular weight, and salt content, and the native state seems to recover after quenching to 40 °C (Matsuda et al., 2009). At concentrations less than ~1000 mg/kg, xanthan gum molecules have more freedom to adopt various conformations, including hairpin-like structures, depending on the system conditions. Studies have indicated that at these concentrations, renaturation does not occur through the formation of aggregates. Instead, each individual dissociated chain forms a double helical structure, characterized by the presence of a hairpin-like structure (Bezemer, Ubbink, de Kooker, Kuil, & Leyte, 2002; Merino-Gonzalez et al., 2017; Norton, Goodall, Frangou, Morris, & Rees, 1984; Tomofuji, Matsuo, & Terao, 2022). However, the xanthan gum denaturation and renaturation processes are complex phenomena, which are still not well understood (Matsuda et al., 2009).

Camesano and Wilkinson (Camesano & Wilkinson, 2001) reported that the single helical (no complete renaturation) form is present in pure water, whereas the double helical form is favored in a salt solution. However, heating treatment of xanthan gum in neat water causes the single-stranded helix to break apart, which can reform in the presence of salt. Tomofuji and coworkers (Tomofuji et al., 2022) used viscometry, circular dichroism, and time-resolved small-angle X-ray scattering to

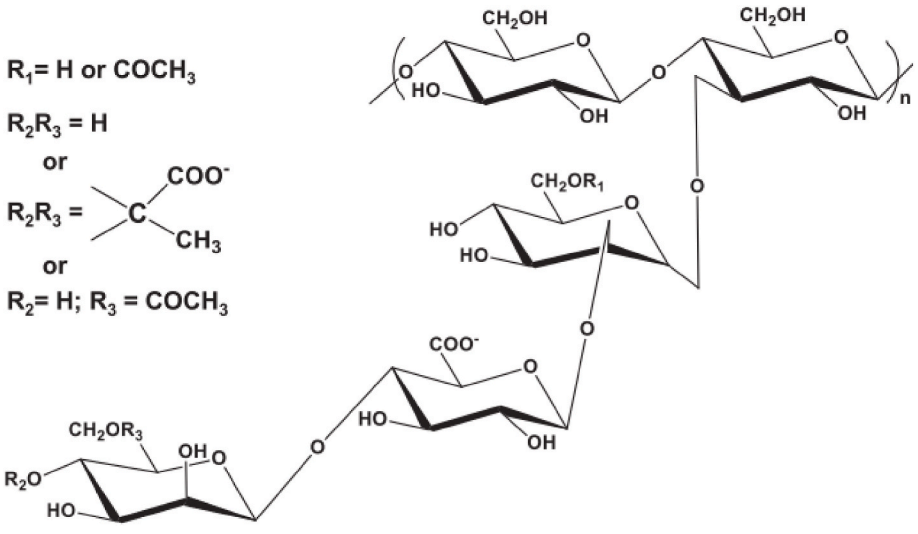


**Fig. 1.** Chemical structure of xanthan gum (Jansson et al., 1975; Melton et al., 1976; Morris, 2019).

study xanthan gum (MW = 341-461 × $10^3$ g/mol) and found a completely ordered structure (renaturation) at 20 °C and a completely disordered (denaturation) at 80 °C. However, Oviatt and coworkers (Oviatt & Brant, 2002) observed that renatured xanthan gum does not recover the native state of the chains in pure water. They used a xanthan gum sample of MW = 0.458–1.20 × $10^6$ g/mol in 0.1 M NaCl, with 0.81 acetyl and 0.59 pyruvyl substitution. Moreover, ordered to the disordered conformation of xanthan gum were found with varied temperatures (20–80 °C) and salt (up to 0.1 M NaBr) employing small angle neutron scattering (Milas Michel, Rinaudo Marguerite, Duplessix Robert, Borsali Redouane, & Peter, 2002). Recently, Brunchi and coworkers (Brunchi et al., 2019; Brunchi, Bercea, Morariu, & Dascalu, 2016) investigated the conformational change of xanthan gum (MW = 1.16 × $10^6$ g/mol) at low ionic strength with a combination of viscometry and spectroscopy, and found that the temperature influenced the conformation transition. The flexible structure of xanthan gum gives higher viscosity than the rod-like structure because the flexible random coil structures can trap more water molecules within its structure, leading to a higher hydrodynamic volume and viscosity than a more ordered structure (Banerjee et al., 2009; Morris et al., 1977). Still, there is no clear explanation why the flexible structure gives higher viscosity than the rod-like structure.

Considering the literature on xanthan gum, the details of how a sample is handled prior to measurement (or used in an application), what treatment and/or pretreatment might have been implemented, etc., can have an impact on the resulting aqueous xanthan gum solution. The processing history can influence molecular arrangements and play a pivotal role in the ensuing solution structure. For example, in polymer processing, thermal annealing often governs the material behavior and therefore its potential applications. To that end, we questioned what might be the effect of repetitive heating and cooling on the polysaccharide xanthan gum. Norton and coworkers (Norton et al., 1984) found no thermal hysteresis between heating and cooling of xanthan gum solution (no molecular weight reported, [xanthan gum] = 2.5 mg $mL^{-1}$) at an elevated temperature (~100 °C). Milas and Rinaudo (Milas et al., 1979) found no hysteresis when investigating using optical rotation the helix-coil transition in the presence of NaCl solution as a function of temperature. On the other hand, Liu and coworkers (Liu, Sato, Norisuye, & Fujita, 1987) observed thermal hysteresis in 0.01 M NaCl that diminished with increased salt concentration. Moreover, Shatwell et al. (Shatwell, Sutherland, Dea, & Ross-Murphy, 1990) found thermal hysteresis of xanthan gum (no molecular weight reported, [xanthan gum] = 0.3% w/w, using polarimetry at 10–90 °C in salt-free solution, and a decrease in the extent of hysteresis with the addition of salt, up to 30 mM NaCl.

The inconsistencies between these studies indicate that it is unclear whether solutions of xanthan exhibit thermal hysteresis. To the best of our knowledge, there are no recent articles on the thermal hysteresis of xanthan gum in aqueous solution. For this reason, our current results contribute to building a more cohesive picture in the literature on the effects of hydrocolloid sample heating and equilibration. In this study we address the following open questions: (1) Is there any thermal history in xanthan gum solutions? (2) What happens to the viscosity when a xanthan gum solution is subjected to heating and controlled rate cooling cycles?

## 2. Experimental

### 2.1. Materials and sample preparation

The xanthan gum used in this study is commercially available (CPKelco, Atlanta, GA, material number: 10040281, CAS: 11138-66-2; E415, food grade, with an estimated molecular weight of 2 × $10^6$ g/mol and polydispersity index ~ 2 (Wyatt & Liberatore, 2009; Wyatt et al., 2010)). The polymer was received in powder form and used without further purification or modification. Deionized water used was purified with a MilliQ system with a measured resistance of 18.2 MΩ cm. A 1600 mg/kg xanthan gum stock solution was prepared by dispersing dried xanthan gum in deionized water. The solution was gently stirred overnight. We meticulously examined the solution for any visual signs of inhomogeneity such as residues, precipitation, lumps, or fisheyes (xanthan agglomeration) and observed uniform solutions. The solution was kept refrigerated at 4 °C to minimize bacterial growth, but was equilibrated at room temperature, 22 °C for 1 h prior to measurement. Appropriate volumes of the xanthan gum stock solution were micropipetted into deionized water to prepare the desired xanthan gum solution concentrations (16, 80, and 320 mg/kg). All samples were prepared from the same batch of xanthan gum powder. Moreover, we limited our experimental concentrations to not more than ~0.3 g/L (= 300 mg/kg) to ensure Newtonian behavior, which has been reported for xanthan gum concentrations below 0.5 g/L (de Moura & Moreno, 2019; Milas & Rinaudo, 1986; Wyatt et al., 2009).

### 2.2. Instrumentation and measurements

Density and viscosity of aqueous xanthan gum at each solution concentration were measured with an Anton-Paar (Anton-Paar-Str. 20, A-8054, Graz, Austria) integrated density/viscosity unit that combines a DMA4100 density meter and Lovis 2000 ME rolling ball viscometer using a quartz capillary (Mat. No. 73109, 1.59 mm) and associated steel ball (1.5 mm diameter and 7.67 g/$cm^3$). Viscometer rolling angles were accurate to ±0.1° and were automatically set by the instrument. Temperature was maintained at ± 0.02 K. Quartz capillaries were calibrated using ultrapure water from Anton Paar. For all viscosity measurements, the uncertainty as at most ±0.2% and reproducibility variation was less than ±0.6%.

Solutions for measurement were prepared by diluting a 1600 mg/kg stock solution to the desired concentration and equilibrated at room temperature. Density and viscosity were measured over a temperature range of 10–70 °C, at increments of 5 °C. For a typical measurement, the sample was held at each temperature for ~15 min during which density and viscosity were measured. No less than six replicate measurements were performed at each temperature, and the reported values represent an average of these replicates.

To investigate the temperature effect on the solution viscosity and density in water, we used two approaches to control cycling through the temperature range, termed “sawtooth” and “triangle”, as illustrated in Fig. 2. The sawtooth pattern consisted of heating the sample incrementally, in 5 °C steps, to a maximum temperature followed by cooling in a single step back to the starting temperature. With the sawtooth approach, cooling to the initial temperature occurred at a rate governed by the speed of the Peltier device, ~2 °C per min. In a parallel set of experiments, samples were heated to the maximum temperature at the same rate but were then cooled in 5 °C steps back to the original temperature prior to beginning the next heating cycle, hence the triangle pattern. For the triangle method, cooling occurred at the same rate as heating, which was controlled by the time required to perform the replicate measurements at each temperature step, ~0.2 °C per min. Shatwell et al. (Shatwell et al., 1990) used a similar approach of heating and cooling of xanthan gum solution in order to determine whether thermal hysteresis was present in the solution.

## 3. Results and discussion

### 3.1. Thermal history

Temperature, alongside of xanthan gum solution concentration, is a factor that influences the macromolecular conformation and association of xanthan gum in solution. Three xanthan gum concentrations were selected that represent the general range of concentrations that have been reported in the literature. Temperature dependent viscosities were measured for each of the solution concentrations and a representative

**Fig. 2.** Schematic representation of heating (red arrows) and cooling (blue arrows) patterns used for viscosity cycles. Sawtooth (left) and triangle (right) patterns are shown for two cycles.

set of replicate viscosities for 16 mg/kg and 320 mg/kg are shown in the upper panels of Fig. 3. For completeness, in Fig. S1 we present the average viscosities for all concentrations measured. The spread in replicate viscosities for the freshly prepared, *non-cycled*, 16 mg/kg xanthan gum solution at 20 °C yielded a 5.4% relative standard deviation (% rsd), which was similar for other temperatures. Replicates at 20 °C for the 320 mg/kg solution showed a slightly lower value of 4.1% rsd, and the viscosity scatter at the higher temperatures remained at ~4% rsd. From this we infer that, on average, it appears that more concentrated xanthan gum solutions yielded more consistent solutions, as evidenced by the slightly lowered % rsd. This perhaps suggests that the solution organization at higher xanthan concentration produces a narrowed distribution of molecular environments. Probabilistically speaking, it makes sense to consider that at higher xanthan concentrations the number of entanglements between xanthan gum chain interactions should increase as the xanthan-xanthan interactions increase. As a side note, we have used time-resolved fluorescence anisotropy (data not shown here but will be reported in due course) to measure solute rotational dynamics and we note that there is an observable difference in dynamics as xanthan concentration is increased. In non-saline xanthan gum solutions at temperatures below 30 °C, xanthan gum chains are partially ordered in a randomly broken helical conformation, expanded because of electrostatic repulsions between charges on the side chains. The transition from a helix to coil-like configuration is suggested to occur because of structural dissociation at higher temperature (Rochefort & Middleman, 1987).

We have computed internal viscosity ratios by normalizing to an upper temperature viscosity with the purpose of examining the viscosity data for variation inconsistencies. The lower panels in Fig. 3 present these results and from these data we observe two points. First, for a given solution composition the internal ratios are consistent across the temperature range studied, with no variation in the temperature pattern except for what is accounted for by uncertainty. Second, on increasing xanthan gum concentration from 16 mg/kg to 320 mg/kg, we observe no significant change ($p < 0.001$) in either the pattern or the relative value. This demonstrates that although the absolute viscosity increases, the temperature change affects freshly prepared xanthan gum solutions in virtually the same way, independent of concentration. Pelletier and coworkers (Pelletier, Viebke, Meadows, & Williams, 2001) found that a 1% xanthan gum in the absence of electrolyte at 25 °C adopts an ordered conformation. As a result, the xanthan gum presents a low viscosity in dilute solution. The transition kinetics from a disordered to ordered conformation is very slow in aqueous solution when a heated solution (range of 40–80 °C) is followed by rapid cooling (to 4 °C) (Bercea et al., 2020).

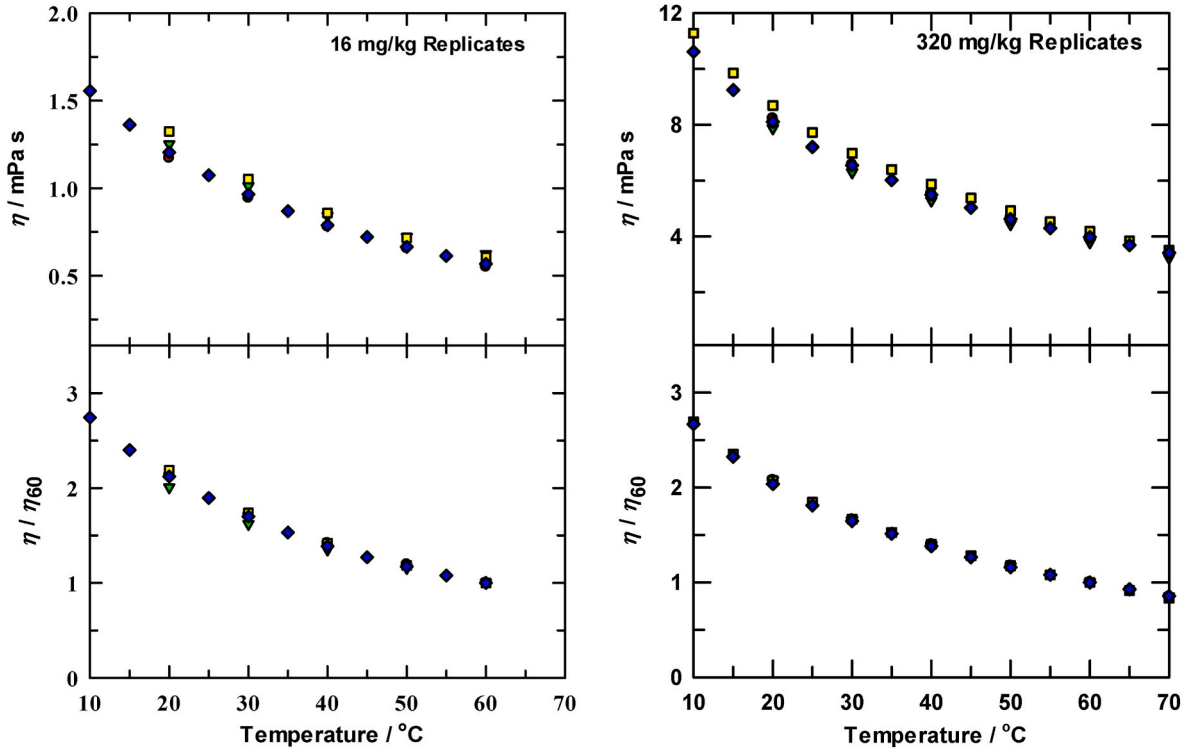


**Fig. 3.** Temperature dependence of aqueous xanthan gum solution viscosities at two xanthan gum concentrations, 16 mg/kg (left panels) and 320 mg/kg (right panels) for freshly prepared replicate samples. Upper panels show the viscosity and lower panels show the internal ratios for each independent data set, normalized to an upper temperature value.

### 3.2. Heating pattern

Having characterized the general behavior of these solutions, we turned our attention to the question of xanthan gum solution performance, with respect to repetitive heating (and cooling) cycles. The transition from a helix to coil motif in xanthan gum as a function of temperature and salt concentration is well documented (Brunchi et al., 2014; Choppe, Puaud, Nicolai, & Benyahia, 2010; Tomofuji et al., 2022; Wyatt, Gunther, & Liberatore, 2011). For the solutions studied here, we limited our investigation to concentration and temperature effects. At the lowest xanthan gum concentration, 16 mg/kg, the "sawtooth" approach (Fig. 2) was performed by heating from 10 °C to 70 °C, followed by direct cooling in a single step to 10 °C, after which the next measurement cycle was initiated. The rate of cooling was governed by the instrument's temperature controller as it reset to the initial value for the next heating cycle. In our case, it took 30 min to cool from 70 °C to 10 °C, which is a cooling rate of 2.0 °C $min^{-1}$. The left panels of Fig. 4 capture the results from these viscosity measurements. The basic temperature pattern is clearly observed, but more importantly we observe a systematic diminution of the xanthan gum viscosity between subsequent heating cycles. On the first heating, the freshly prepared sample produced the highest viscosity values at each temperature ●. The second heating cycle showed the most significant viscosity decrease compared to the remaining cycles (see for example, ▼ at 10 °C in Fig. 4).

Solutions were also characterized by plotting the viscosity at constant temperature for the heating cycles. In this way, we could examine the relative change to determine how the temperature contributed to the viscosity change upon subsequent heating cycles. Representative examples of the viscosity changes in 16 mg/kg xanthan gum at selected temperatures are shown in the left panel of Fig. 5 for the "sawtooth" heating pattern as the number of cycles is increased. Lines in this plot are regressions to these data using a second order polynomial, and the polynomial fitting parameters are reported in Table 1. For the "sawtooth" heating (Fig. 5, left panel), the quadratic coefficient "*a*" showed a notable decrease in value as temperature increased, indicating a flattening of the curvature. Applying replicate heating cycles to the solution at low temperature (10 °C, Fig. 5) shows a more pronounced effect compared to replicate cycles at higher temperature (55 °C, Fig. 5). Capron and coworkers (Capron et al., 1997) reported that xanthan gum chain rigidity decreased with increasing temperatures above 50 °C, which is consistent with the denaturation temperature range. No hysteresis was observed by re-cooling the samples to 25 °C after heating to 70 °C. However, our data do show a clear viscosity dependence on heating, giving indication that the xanthan gum solutions may not be as robust with respect to repetitions of thermal cycles.

In support of this observation, the left panel of Fig. 6 shows the computed % change in viscosity for the "sawtooth" heating pattern in 16 mg/kg xanthan gum at all temperatures measured. We observed an initial viscosity decrease of about 7% at 10 °C (red bars) between heating cycle 1 and 2, which systematically diminished to 2.5% at 60 °C, suggesting that the subsequent structural relaxation was less impactful at higher temperature. The viscosity decrease between heating cycles 2 and 3 (green bars) was significantly smaller at lower temperatures and held relatively constant at ~2–3%. Once again, for heating cycle 3 to 4 (yellow bars) there was a further decrease in viscosity that remained constant at ~1.5%. As a final comparison, we computed the overall % change between cycle 1 and 4 and observed that at 10 °C the viscosity lowered by about 10%. At 60 °C, the overall change lessened to only 8%.

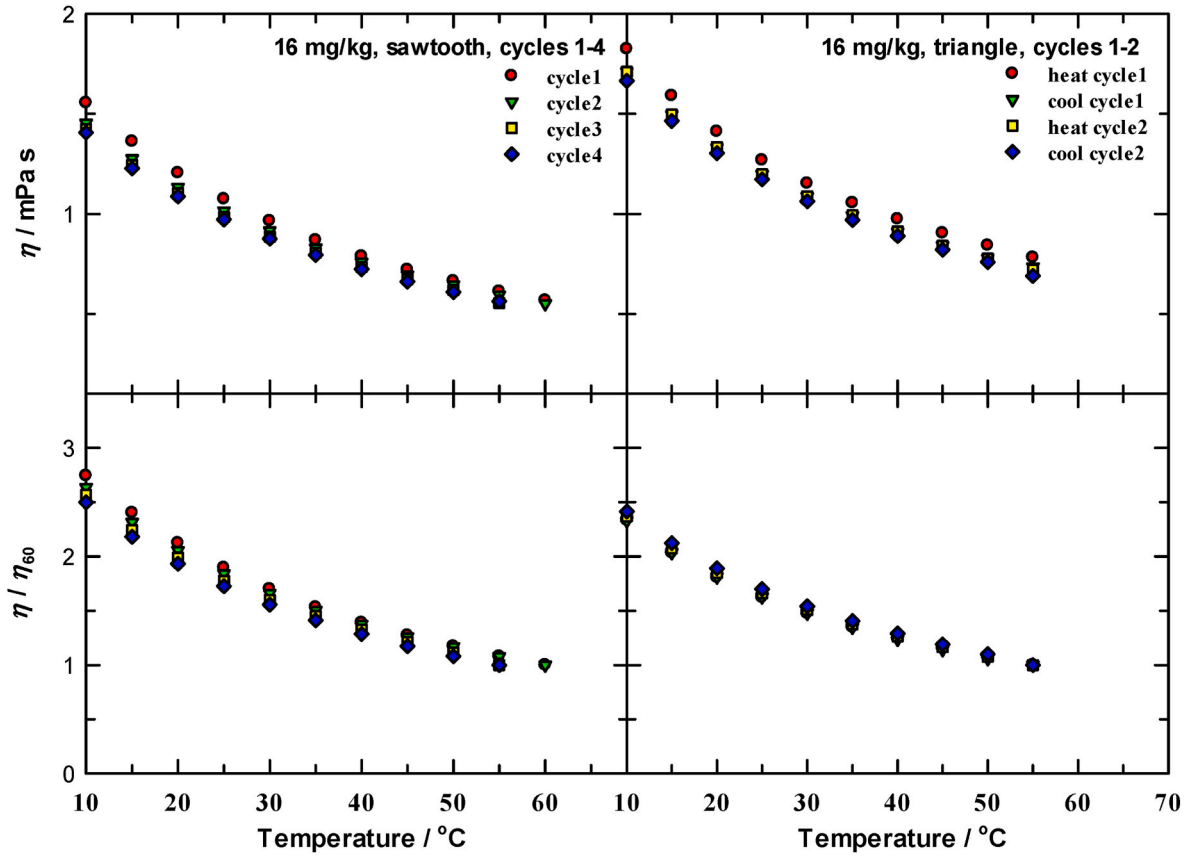


**Fig. 4.** Left panels plot the viscosity as a function of temperature for 16 mg/kg xanthan gum in water using the "sawtooth" pattern. The upper panel is the viscosity, and the lower panel is the corresponding internal viscosity ratio for each independent cycle. Cycle repetitions are shown in sequence as "sawtooth" heating. Right panels show the "triangle" thermal cycling for viscosity (upper panel) and the internal ratios (lower panel). Note that the "triangle" sequence is for heating/cooling pairs, here for two complete cycles.

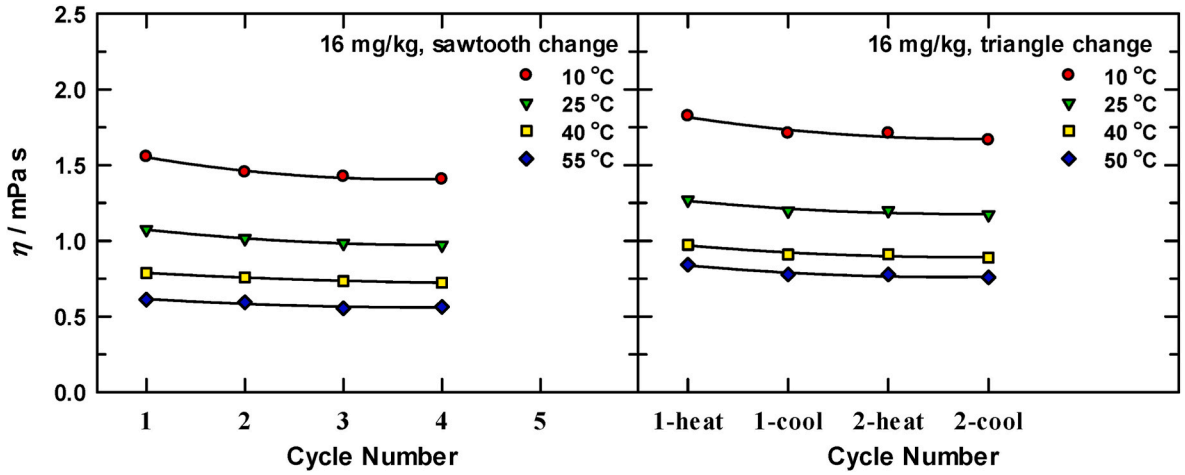


**Fig. 5.** Observed viscosity changes in 16 mg/kg xanthan gum solutions, for the "sawtooth" (left) and "triangle" (right) patterns, respectively. The four "sawtooth" cycles are sequential heating only cycles whereas the four "triangle" cycles represent heating-cooling-heating-cooling. Lines are fits to a second order polynomial and used only to assess relative curvature. Fitting results are reported in Table 1.

**Table 1**
Coefficients from polynomials fits to viscosities at selected temperature for 16 mg/kg, 80 mg/kg, and 320 mg/kg xanthan gum aqueous solutions.

| | Sawtooth Cycles | | | Triangle Cycles[a] | | |
|---|---|---|---|---|---|---|
| 16 mg/kg Aqueous Xanthan Gum Solution | | | | | | |
| T/°C | a | b | c | a | b | c |
| 10 | 0.021 ± 0.007 | −0.15 ± 0.04 | 1.69 ± 0.04 | 0.017 ± 0.018 | −0.13 ± 0.09 | 1.93 ± 0.10 |
| 25 | 0.012 ± 0.001 | −0.092 ± 0.006 | 1.15 ± 0.007 | 0.012 ± 0.011 | −0.09 ± 0.06 | 1.34 ± 0.06 |
| 40 | 0.004 ± 0.001 | −0.044 ± 0.004 | 0.83 ± 0.004 | 0.011 ± 0.010 | −0.08 ± 0.05 | 1.04 ± 0.06 |
| 55 | 0.006 ± 0.008 | −0.05 ± 0.04 | 0.66 ± 0.04 | 0.012 ± 0.009 | −0.08 ± 0.05 | 0.91 ± 0.05 |
| 80 mg/kg Aqueous Xanthan Gum Solution | | | | | | |
| 10 | 0.087 ± 0.008 | −0.729 ± 0.039 | 3.76 ± 0.043 | 0.036 ± 0.088 | −0.42 ± 0.45 | 3.79 ± 0.49 |
| 25 | 0.062 ± 0.007 | −0.512 ± 0.037 | 2.58 ± 0.04 | 0.027 ± 0.058 | −0.30 ± 0.30 | 2.60 ± 0.32 |
| 40 | 0.042 ± 0.008 | −0.339 ± 0.041 | 1.88 ± 0.045 | 0.034 ± 0.037 | −0.28 ± 0.19 | 1.97 ± 0.21 |
| 55 | 0.028 ± 0.007 | −0.238 ± 0.036 | 1.48 ± 0.039 | 0.018 ± 0.016 | −0.16 ± 0.08 | 1.49 ± 0.09 |
| 320 mg/kg Aqueous Xanthan Gum Solution | | | | | | |
| 10 | 0.19 ± 0.037 | −1.91 ± 0.19 | 13.02 ± 0.21 | −0.05 ± 0.22 | −0.32 ± 1.1 | 10.9 ± 1.2 |
| 25 | 0.13 ± 0.023 | −1.28 ± 0.12 | 8.89 ± 0.13 | −0.05 ± 0.13 | −0.12 ± 0.66 | 7.3 ± 0.73 |
| 40 | 0.17 ± 0.011 | −1.34 ± 0.06 | 7.05 ± 0.06 | 0.04 ± 0.10 | −0.49 ± 0.51 | 5.9 ± 0.56 |
| 55 | 0.08 ± 0.14 | −0.78 ± 0.71 | 5.22 ± 0.77 | −0.02 ± 0.14 | −0.22 ± 0.71 | 4.5 ± 0.77 |
| 7 cycle heating only regressions | | | | | | |
| 10 | | | | 0.097 ± 0.012 | −1.32 ± 0.10 | 11.9 ± 0.17 |
| 25 | | | | 0.060 ± 0.008 | −0.85 ± 0.07 | 8.0 ± 0.12 |
| 40 | | | | 0.049 ± 0.004 | −0.66 ± 0.03 | 6.08 ± 0.06 |
| 55 | | | | 0.04 ± 0.004 | −0.54 ± 0.03 | 4.78 ± 0.06 |

[a] Triangle regressions at each temperature included data from heat 1, cool 1, heat 2, and cool 2 cycles.

Although we cannot describe the specific xanthan gum structural organization from these measurements, it is evident that a freshly prepared solution undergoes a structural change that is driven by temperature and that repeat heating continues to induce structural change that does not recover upon returning to the initial temperature. Bercea et al. (Bercea et al., 2020) reported that all xanthan gum chains are in a disordered (random coil) state at 80 °C and its recovery time is slower. The ordered structure recovery time occurs more rapidly at 40 °C since the macromolecules are in a partially disordered state and the entropy difference between the two states is smaller. Following the fourth cycle, we measured the viscosity at 20 °C only with no further heating at intervals of 3, 6, 10, and 24 h and found that the viscosity remained constant at $1.071_6 \pm 0.003_4$ mPa s.

To further probe the thermal effects on the xanthan gum solution viscosity, we questioned whether there might be an unobserved contribution to the xanthan gum structure by rapidly cooling from the final temperature back to 20 °C such as an annealing effect. How does the xanthan gum solution viscosity change with denaturation (disrupting the chain organization, and is there any conformational recovery (renaturation of the chains)? These questions led us to measure viscosity not only as a function of heating but also to track viscosity under a slower cooling rate, the "triangle" pattern (Fig. 2). By stepping down in 5 °C increments, it took 300 min to cool from 70 to 10 °C, which is a rate of 0.20 °C $min^{-1}$ and a factor of 10 slower than for the "sawtooth" data. Right side panels in Fig. 4 (cycle viscosities), Fig. 5 (constant temperature viscosities), and Fig. 6 (cycle-to-cycle % change) show the results from these experiments. Overall, we observe the same general patterns as the heating-only data, but the "triangle" viscosities and ratio values appear to show a bit more fluctuation. The viscosities in cooling cycle 1 (▼) decreased at all temperatures compared to the first heating cycle. Interestingly, the cooling values in cycle 1 were identical to the heating values in cycle 2 (▼and ■), to within uncertainty. This is made clear in the % change data (see Fig. 6, green bars). As with the heating only experiment, the viscosity *difference* between the adjacent heating cycles

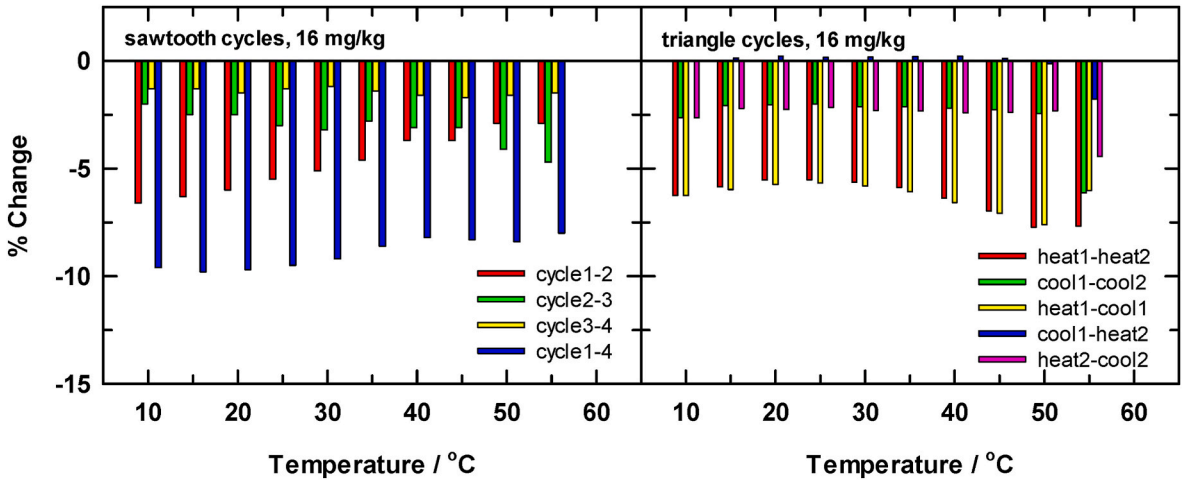


**Fig. 6.** Percent viscosity changes between subsequent thermal cycles in 16 mg/kg xanthan gum solutions, for the "sawtooth" (left) and "triangle" (right) patterns, respectively.

consistently diminished (Fig. 4, ● and ■). The computed "triangle" viscosity ratios indicate a more uniform viscosity change for 16 mg/kg xanthan gum across the two heating and cooling cycles when a controlled cooling rate is implemented. While it may appear from these ratios that including a cooling cycle has a normalizing effect, comparing the % change between heating cycles 1 and 2, red bars in each panel of Fig. 6, it does not appear that the viscosity change is significantly different and remains within ~7% over the temperature range. What does appear to be impacted is the low temperature viscosity variation over replicate heating. The viscosity change cycle-to-cycle when cooling is included, right panel of Fig. 5 and in Table 1, shows less curvature over all temperatures and in fact, the quadratic coefficient uncertainties suggest that $a$ is statistically zero so that a linear model appears to suffice to describe the viscosity variation at each temperature. Brunchi and coworkers (Brunchi et al., 2019) noted that the intermolecular associations based on the hydrogen bonds were disrupted at temperature up to 37 °C. However, increasing to temperature up to 50 °C caused the hydrogen bonds among the side chains and backbone to break down. Thus, the side chains move freely in solution and initiate the order-disorder state transition which, in return, results in high solution viscosity.

To summarize, in 16 mg/kg xanthan gum aqueous solution subsequent heating cycles by either cycling pattern shows that the xanthan gum solution viscosity *does not* recover the initial value, indicating that the thermal denaturation effect is irreversible. Moreover, the inclusion of slow cooling does not stave off structural denaturation. We did note that, when comparing a cooling cycle viscosity to the next heating cycle viscosity, there was effectively no change in value (blue bars in the right panel of Fig. 6). This suggests that controlled cooling does not affect the xanthan gum denaturation, nor does it improve structural renaturation at least in dilute xanthan gum solution. Prolonged equilibration at room temperature (>24 h) was also ineffective at recovering the viscosity value of the freshly prepared solution.

### 3.3. Concentration effects

Having characterized the temperature effect on viscosity in dilute xanthan gum solution, we turned toward studying the effect of increasing xanthan gum concentration. We repeated all experiments for 80 mg/kg and 320 mg/kg xanthan gum solutions and the viscosities are presented in Fig. S2 and Fig. S3, respectively. The overall viscosity patterns in these solutions display the same general features as described for 16 mg/kg xanthan gum, and the viscosity ratios cycle-to-cycle are the same to within experimental uncertainty. When examining the constant temperature viscosity data summarized in Fig. S4 and Fig. S5, we note several points. First, increasing temperature for a fixed concentration always decreased the absolute viscosity with a concomitant decrease in curvature (see also Table 1). With increased concentration, the degree of curvature appeared to weaken. For example, in 80 mg/kg xanthan gum the $a$ parameter decreased by three-fold and 320 mg/kg xanthan gum decreased by 2.5. Second, higher concentration xanthan gum solutions showed greater curvature, particularly at the lower temperatures where $a$ is substantially larger. We observed a four-fold increase in $a$ at 10 °C on increasing concentration from 16 mg/kg and 80 mg/kg and a 9-fold increase for 16 mg/kg to 320 mg/kg. At 55 °C the change is even greater, where we observe a 13-fold increase in curvature between 16 mg/kg and 320 mg/kg. Clearly, at higher concentration the structural organization is more extensive and complex and with increased fluidity the variety of chain interactions and dynamics contributes to the greater magnitude of viscosity change. However, from viscosity alone we cannot infer what other/additional specific structural changes may be taking place to mitigate viscosity. We also consider the "triangle" patterns and note that with a lesser number of heating cycles we are not able to assess viscosity change in a way that is strictly comparative to what the heating only ("sawtooth") pattern indicates.

Care must be taken when evaluating the "triangle" plots because, while the cycle repetition data may suggest slight curvatures in the viscosity, the cooling cycle viscosities are consistently less than the preceding heating cycle and are essentially equal to the subsequent heating cycle. This results in a nulling effect of the viscosity curvature with respect to cooling offsetting heating in adjacent cycles. From a statistical perspective, the $a$ parameters and uncertainties listed in Table 1 are zero, and a second order polynomial model is not justified. We also see that for "triangle" data at all xanthan gum concentrations in Fig. S6, the heat1-cool1 viscosity change (yellow bars) is the same as for the heat1-heat2 viscosity change (red bars). On examining the end of the second heating cycle for both experiment patterns, we observe that the relative decrease in % change is similar in both patterns and is on the order of ~5% ("sawtooth" pattern, red to green bars and "triangle" data, red to purple bars) for 16 mg/kg xanthan gum.

It is interesting to note that for 80 mg/kg and 320 mg/kg xanthan gum solutions that the % change for the first heating cycle was between 10 and 15%, which is larger than the case of 16 mg/kg by a factor of two (red bars). The second heating cycle (green bars and purple bars for "sawtooth" and "triangle", respectively) at higher concentrations continued to follow the same trend as in 16 mg/kg and showed less change but the relative change was not as great. The 320 mg/kg solution seems to show the least difference in % change, which suggests that higher xanthan gum concentrations seem to be more stable with respect to thermal denaturation. According to Camesano et al. (Camesano et al.,

2001), the double helix of xanthan gum in pure water does not fully re-form.

To ascertain a better understanding of the cooling contribution (if any) and to better compare to the "sawtooth" data, we repeated the "triangle" pattern experiment at 320 mg/kg to include seven complete heating/cooling cycles. Fig. 7 summarizes the viscosity at representative temperatures for the seven "triangle" heating cycles. The general pattern of decreasing viscosity with temperature *and* replicates at constant temperature is clear. At about cycle 6, there is a distinct decrease in relative change within a temperature set. It seems that six or seven heating cycles are required before the rate of viscosity change slows to what appears to be a plateau value. This seems most obvious at higher temperature (e.g., 55 °C, ◆ symbols) compared to lower temperature (e.g., 10 °C, ● symbols). We also computed the % change and that data is presented in Fig. 8. By the sixth or seventh cycle, the % change has diminished to about 2.5% change, similar to what was observed in 16 mg/kg xanthan gum after only four heating cycles.

The structure formed in 320 mg/kg xanthan gum concentration requires more heating cycles to achieve the same level of apparent relaxation (denaturation) as indicated by the overall change that occurs as a function of concentration (blue bars in Fig. S6 for all "sawtooth" concentrations). For 16 mg/kg xanthan gum, we observe at most a 10% change in viscosity over four heating cycles, with a modest lowering of the change at higher temperatures. On increasing concentration, the overall % change rose to between 25 and 30% in 80 mg/kg xanthan gum, again with a small decrease at higher temperature, and the 320 mg/kg xanthan gum solution remained constant across the temperature range at about 25% change. This further supports the notion that there is much more structural change occurring in higher concentration xanthan gum solutions. When we compare the seven heating cycles for the 320 mg/kg xanthan gum solution, we observe a uniform 30% change in viscosity across temperature. It is further possible to consider that, due to the increased viscosity of solutions at higher temperatures, xanthan gum molecules are moving slower and, therefore, take longer to rearrange. Indeed, there is an inverse correlation between the solution viscosity and the diffusion coefficients, $D$, of polysaccharides:

$$D\ \left(cm^2 s^{-1}\right) = 8.34 \times 10^{-8} \frac{T}{\eta (M_w)^{1/3}} \quad (1)$$

where $\eta$ is solution viscosity, $T$ is temperature, and $M_w$ is polysaccharide molecular weight (Masuelli, 2011). While we can estimate the apparent diffusion coefficient to show that the rearrangement kinetics are slowed as a function of both temperature and concentration (for completeness we include these data in Fig. S7), it is true that using either viscosity or diffusion coefficients to express the observed solution changes results in the same end statement.

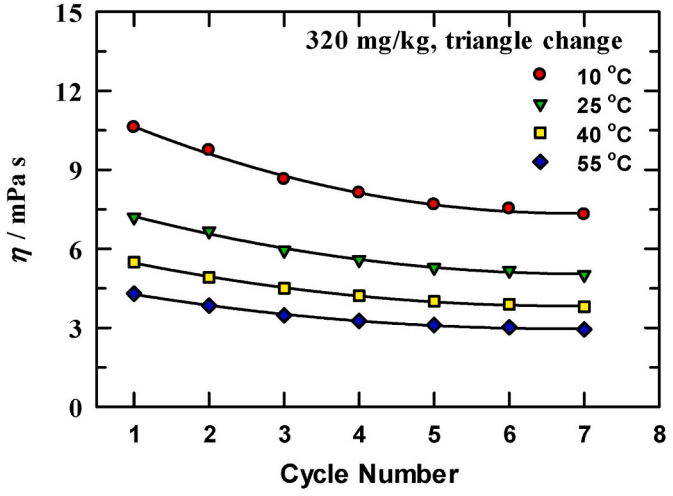


**Fig. 7.** Viscosity as a function of the number of heating/cooling cycles for representative temperatures for 320 mg/kg xanthan gum in salt-free water. Cycle repetitions are shown in sequence as heating only for the "triangle" pattern.

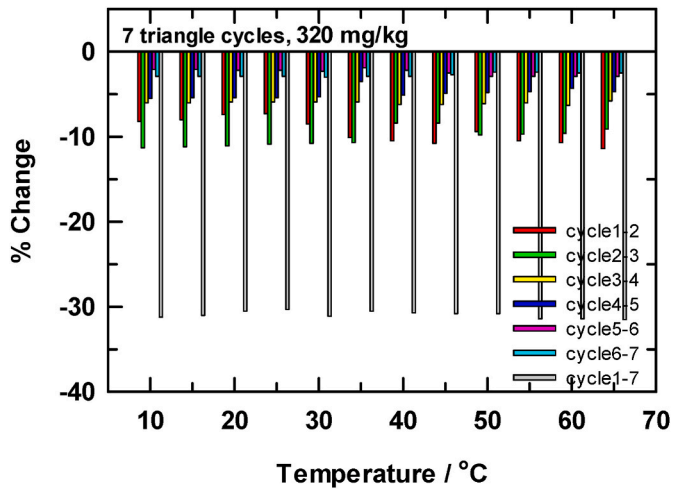


**Fig. 8.** Percent viscosity changes between for seven thermal cycles in 320 mg/kg aqueous xanthan gum solution for the "triangle" pattern.

### 3.4. Activation energy

For polysaccharides like xanthan gum, the network structure is disrupted by the increasing temperature of the aqueous media. The effect of temperature on xanthan gum solution viscous flow was characterized by using the Arrhenius equation:

$$\ln(\eta) = \ln(A) + E_a/RT \quad (2)$$

where $E_a$ represents the energy required by molecules to flow at various temperatures at zero-shear viscosity when the material is at rest, $A$ is a pre-exponential factor, $R$ is the universal gas constant (8.314 J/mol K), and $T$ is the absolute temperature. A higher value of $E_a$ indicates that the solution is more sensitive to temperature, and the polymer chain backbone is more prone to conformational change (Xu, Xu, Liu, Chen, & Gong, 2013). The $E_a$ values were calculated from the slopes of

**Table 2**
Activation energies from viscosities for 16 mg/kg, 80 mg/kg, and 320 mg/kg xanthan gum aqueous solutions.

| 16 mg/kg | | | |
|---|---|---|---|
| | Sawtooth Cycles | Triangle Cycles[a] | First Run Averages |
| Cycle | Ea | Ea | |
| 1 | 15.8 ± 0.2 | 14.1 ± 0.3 | 15.0 ± 0.3 |
| 2 | 15.1 ± 0.2 | 15.1 ± 0.4 | |
| 3 | 15.8 ± 0.2 | 15.0 ± 0.4 | |
| 4 | 15.6 ± 0.2 | 15.3 ± 0.3 | |
| 80 mg/kg | | | |
| 1 | 14.7 ± 0.5 | 15.6 ± 0.3 | 14.8 ± 0.5 |
| 2 | 14.4 ± 0.5 | 16.7 ± 0.8 | |
| 3 | 13.8 ± 0.5 | 16.2 ± 0.7 | |
| 4 | 13.7 ± 0.4 | 13.9 ± 0.6 | |
| 320 mg/kg | | | |
| 1 | 15.2 ± 0.3 | 15.1 ± 0.3 | 15.0 ± 0.3 |
| 2 | 15.0 ± 0.3 | 15.7 ± 0.3 | |
| 3 | 14.9 ± 0.3 | 15.6 ± 0.3 | |
| 4 | 14.8 ± 0.3 | 15.5 ± 0.4 | |

[a] Triangle cycle activation energies are reported in the order of heat 1, cool 1, heat 2, and cool 2.

experimental data and summarized in Table 2. Our values are in good agreement with the literature reports of 14.7 kJ/mol (Brunchi, Bercea, Morariu, & Dascalu, 2016) and 15.3 kJ/mol (Banerjee et al., 2009). We also compared our xanthan gum activation energies with data from guar gum determinations and found that the xanthan gum values are about 45% lower than for guar gum 27.2 kJ/mol (Wang, He, Guo, Zhao, & Tang, 2015). Xanthan gum energies were also less than chemically modified guar gum energies, 30% lower than O-carboxymethyl-O-hydroxypropyl guar gum (22.0 kJ/mol), 21% less than O-carboxymethyl-O-2-hydroxy-3-(trimethylammonio) propyl guar gum (19.4 kJ/mol), and 17% less than O-2-hydroxy-3-(trimethylammonio) propyl guar gum (18.0 kJ/mol) (Zhang, Zhou, & Hui, 2005). Given the flatter slopes in xanthan gum, this suggests that the backbone fluctuations of the xanthan gum chain are less sensitive to temperature variations than guar gum and its derivatives. Moreover, xanthan gum solutions show a lower barrier to molecular transport by virtue of its reduced energy barrier to initiating flow thus enhancing its utility in chemical applications. The consistent $E_a$ values show that the hydrogen bonding-induced network structure is less likely to collapse as the temperature increases (Brunchi, Bercea, Morariu, & Dascalu, 2016; Wang et al., 2015).

### 3.5. Density

To further characterize the influence of thermal cycles on the xanthan gum solutions, we measured density as a function of concentration, temperature, and cycling pattern to assess the effect of changes on solution volume. Density data are compiled in Table S1 for averages of at least three replicates of freshly prepared solutions of 16, 80, and 320 mg/kg xanthan gum. We observed consistent results over all temperatures and for all xanthan gum concentrations as shown in Fig. S8 (upper panel), which also includes neat water for comparison. Shown in the lower panel is an example of the individual replicate agreement for 80 mg/kg xanthan gum. For the 16 and 80 mg/kg xanthan gum solutions, the density values of the replicates at each temperature were in exact agreement to four significant figures, with a relative standard deviation of zero. The 320 mg/kg solutions were nearly as good showing only about 0.03% relative standard deviations. In this regard, the replicate density results are similar to viscosity in that the main reproducibility limitation was that of instrumental precision. When only heating was applied with no cycling, repeated measurement results were in excellent agreement and, as expected, the density systematically decreased with increasing temperature as the solution volume expanded. This clearly correlates with a decreased bulk viscosity. What is most interesting here and important to note is that no matter the xanthan gum concentration, the results did not deviate significantly from the neat water density. If we presume that the xanthan gum structure is in the more tightly packed helical conformation, then these data suggest that the bulk solution is unperturbed by the presence of xanthan gum at each of the reported concentrations.

Also reported are the density data for the sawtooth and triangle cycled measurements. Thermally cycled density measurements paralleled the observed viscosity pattern and showed that subsequent cycles after the first run produced systematically lowered densities with repeated cycles. Fig. S9 summarizes examples of these data for sawtooth (upper panel) and triangle (lower panel) cycling. We noted that the most substantial change for the sawtooth data occurred between cycle 1 and 2, after which the densities remained consistent to within experimental uncertainty. It appears that the first heating contributed most to structural reorganization within the solution that apparently remained consistent on subsequent cycles. The lowered density at a given concentration and temperature suggests an expanded solution structure, akin to a looser coil-like structure that would be consistent with the reported with a change from a helical conformation to random coil motif. This effect is independent of the cycling method and in comparison, the triangle approach showed the same behavior. However, the slowed, systematic cooling rate seems to have an additional contribution to lowering the solution density. Density data show that there is a clear decrease in density between heating cycles, but the cooling side of the pattern produced a further reduced density. We also note that this behavior is consistent across all concentrations measured here, with 16 mg/kg xanthan gum showing the least impact, and 320 mg/kg xanthan gum showing the greatest effect. Conjecture would suggest that after heating, the structure is modified and a slow cooling rate allows for some degree of additional structural equilibration. From our data here, we are limited in what we may assert about the details of xanthan gum organizational change, but the effect is clear. Moreover, the density data buttress the point made from viscosity measurements in that, once the solutions are denatured from their initial solution state at the beginning of our measurements herein, they do not return to the initial solution values.

## 4. Conclusions

The effect of consecutive heating and heating/cooling cycles on solution viscosity has been measured for 16, 80, and 320 mg/kg xanthan gum in an aqueous, salt-free solution. The influence of heating cycles on the xanthan gum viscosity showed the presence of thermal hysteresis, which depends more strongly on xanthan gum concentration than solution temperature. We observed a concentration dependence that showed the viscosity of the 16 mg/kg solutions decreased by about 6% on the first heating cycle of the sawtooth pattern, which diminished to 1% after the fourth heating cycle. The combined change was 9% overall from cycle 1 to cycle 4. For the 320 mg/kg solutions, there was a decrease of 11% on the first heating cycle, that diminished to 6% by the fourth heating cycle, with a total change of 25% from cycle 1 to cycle 4. The activation energy was constant across concentrations at ~15.0 kJ/mol.

Based on the experimental results, the conclusions can be summarized as follows. (1) Heating following multistep cooling cycles shows modifications on the structure of xanthan gum in solution. When the xanthan gum solution is treated using heating followed by a slow, stepwise cooling cycle, the slowed cooling rate minimized the impact on viscosity change because there was extended time for the system to fully equilibrate. Our data suggest a greater degree of xanthan gum denaturation when using the “sawtooth” pattern. To further clarify, the rate and degree to which we observe renaturation of xanthan gum is directly influenced by the experimental cooling rate given that heating rates were identical in both experimental methods. (2) The original viscosity (of a freshly prepared solution) was never recovered, indicating that the polymer chains do not return to their initial state. This was determined by making additional viscosity measurements after completion of heating/cooling cycles by measuring solution viscosity at 20 °C over a period of 60 h with no return to the original value, that of a freshly prepared solution. The bulk structural transformation to a disordered state, or a more flexible xanthan gum conformation, is supported by these data because of the net decrease in viscosity after repeated heating/cooling cycles. Our data evidence the importance of using a controlled cooling rate to influence the relative rates of xanthan gum renaturation.

## Author statement

Paschalis Alexandridis: Conceptualization, Writing-Original draft preparation, Writing-Reviewing and Editing, Supervision, Project Administration; Emmanuel Nsengiyumva: Methodology, Data curation, Investigation, Formal Analysis, Writing-Original draft preparation, Validation; Mark Heitz: Methodology, Data curation, Investigation, Formal Analysis, Writing-Original draft preparation, Writing-Reviewing and Editing, Validation, Resources, Project Administration.

## Declaration of competing interest

The authors declare that they have no known competing financial interests or personal relationships that could have appeared to influence the work reported in this paper.

## Data availability

Data will be made available on request.

## Acknowledgments

The authors gratefully acknowledge support from the National Science Foundation, award numbers 1953428 and 2216375. Financial support was also provided by SUNY Brockport through the Scholarly Incentive Grant and the Provost Post-tenure Grant programs. EMN was supported in part by the SUNY PRODiG Fellowship program.

## Appendix A. Supplementary data

Supplementary data to this article can be found online at https://doi.org/10.1016/j.foodhyd.2023.108973.

## References

Abbaszadeh, A., Lad, M., Janin, M., Morris, G. A., MacNaughtan, W., Sworn, G., et al. (2015). A novel approach to the determination of the pyruvate and acetate distribution in xanthan. *Food Hydrocolloids, 44*, 162–171. https://doi.org/10.1016/j.foodhyd.2014.08.014

Abu Elella, M. H., Goda, E. S., Gab-Allah, M. A., Hong, S. E., Pandit, B., Lee, S., et al. (2021). Xanthan gum-derived materials for applications in environment and eco-friendly materials: A review. *Journal of Environmental Chemical Engineering, 9*(1). https://doi.org/10.1016/j.jece.2020.104702

Ahmad, M., Ritzoulis, C., Chen, J., Meigui, H., Bushra, R., Jin, Y., et al. (2021). Xanthan gum – mucin complexation: Molecular interactions, thermodynamics, and rheological analysis. *Food Hydrocolloids, 114*. https://doi.org/10.1016/j.foodhyd.2020.106579

Banerjee, P., Mukherjee, I., Bhattacharya, S., Datta, S., Moulik, S. P., & Sarkar, D. (2009). Sorption of water vapor, hydration, and viscosity of carboxymethylhydroxypropyl guar, diutan, and xanthan gums, and their molecular association with and without salts (NaCl, CaCl2, HCOOK, CH3COONa, (NH4)2SO4 and MgSO4) in aqueous solution. *Langmuir, 25*(19), 11647–11656. https://doi.org/10.1021/la901259e

Becker, A., Katzen, F., Puhler, A., & Ielpi, L. (1998). Xanthan gum biosynthesis and application: A biochemical/genetic perspective. *Applied Microbiology and Biotechnology, 50*(2), 145–152. https://doi.org/10.1007/s002530051269

Bercea, M., & Morariu, S. (2020). Real-time monitoring the order-disorder conformational transition of xanthan gum. *Journal of Molecular Liquids, 309*, Article 113168. https://doi.org/10.1016/j.molliq.2020.113168

Bezemer, L., Ubbink, J. B., de Kooker, J. A., Kuil, M. E., & Leyte, J. C. (2002). On the conformational transitions of native xanthan. *Macromolecules, 26*(24), 6436–6446. https://doi.org/10.1021/ma00076a021

Bhat, I. M., Wani, S. M., Mir, S. A., & Masoodi, F. A. (2022). Advances in xanthan gum production, modifications and its applications. *Biocatalysis and Agricultural Biotechnology, 42*. https://doi.org/10.1016/j.bcab.2022.102328

Brunchi, C.-E., Avadanei, M., Bercea, M., & Morariu, S. (2019). Chain conformation of xanthan in solution as influenced by temperature and salt addition. *Journal of Molecular Liquids, 287*, Article 111008. https://doi.org/10.1016/j.molliq.2019.111008

Brunchi, C.-E., Bercea, M., Morariu, S., & Avadanei, M. (2016a). Investigations on the interactions between xanthan gum and poly(vinyl alcohol) in solid state and aqueous solutions. *European Polymer Journal, 84*, 161–172. https://doi.org/10.1016/j.eurpolymj.2016.09.006

Brunchi, C.-E., Bercea, M., Morariu, S., & Dascalu, M. (2016b). Some properties of xanthan gum in aqueous solutions: Effect of temperature and pH. *Journal of Polymer Research, 23*(7), 1–8. https://doi.org/10.1007/s10965-016-1015-4

Brunchi, C. E., Morariu, S., & Bercea, M. (2014). Intrinsic viscosity and conformational parameters of xanthan in aqueous solutions: Salt addition effect. *Colloids and Surfaces B: Biointerfaces, 122*, 512–519. https://doi.org/10.1016/j.colsurfb.2014.07.023

Brunchi, C.-E., Morariu, S., & Bercea, M. (2021). Impact of ethanol addition on the behaviour of xanthan gum in aqueous media. *Food Hydrocolloids, 120*. https://doi.org/10.1016/j.foodhyd.2021.106928

Callet, F., Milas, M., & Rinaudo, M. (1987). Influence of acetyl and pyruvate contents on rheological properties of xanthan in dilute solution. *International Journal of Biological Macromolecules, 9*(5), 291–293. https://doi.org/10.1016/0141-8130(87)90068-7

Camesano, T. A., & Wilkinson, K. J. (2001). Single molecule study of xanthan conformation using atomic force microscopy. *Biomacromolecules, 2*(4), 1184–1191. https://doi.org/10.1021/bm015555g

Capron, I., Brigand, G., & Muller, G. (1997). About the native and renatured conformation of xanthan exopolysaccharide. *Polymer, 38*(21), 5289–5295. https://doi.org/10.1016/s0032-3861(97)00079-7

Chatterji, J., & Borchardt, J. K. (1981). Applications of water-soluble polymers in the oil field. *Journal of Petroleum Technology, 33*(11), 2042–2056. https://doi.org/10.2118/9288-pa

Choppe, E., Puaud, F., Nicolai, T., & Benyahia, L. (2010). Rheology of xanthan solutions as a function of temperature, concentration and ionic strength. *Carbohydrate Polymers, 82*(4), 1228–1235. https://doi.org/10.1016/j.carbpol.2010.06.056

Dumitriu, S. (2005). *Polysaccharides: Structural diversity and functional versatility* (2nd ed. Vol. 29). Portland: Ringgold, Inc.

Faria, S., de Oliveira Petkowicz, C. L., de Morais, S. A. L., Terrones, M. G. H., de Resende, M. M., de França, F. P., et al. (2011). Characterization of xanthan gum produced from sugar cane broth. *Carbohydrate Polymers, 86*(2), 469–476. https://doi.org/10.1016/j.carbpol.2011.04.063

Garcia-Ochoa, F., Santos, V. E., Casas, J. A., & Gomez, E. (2000). Xanthan gum: Production, recovery, and properties. *Biotechnology Advances, 18*(7), 549–579. https://doi.org/10.1016/s0734-9750(00)00050-1

Holzwarth, G. (1978). Molecular weight of xanthan polysaccharide. *Carbohydrate Research, 66*(1), 173–186. https://doi.org/10.1016/S0008-6215(00)83250-4

Jansson, P.-e., Kenne, L., & Lindberg, B. (1975). Structure of the extracellular polysaccharide from xanthomonas campestris. *Carbohydrate Research, 45*(1), 275–282. https://doi.org/10.1016/S0008-6215(00)85885-1

-2008. *KELTROL®/KELZAN® xanthan gum. Book 8th edition* (8 ed., (2001 pp. 1–32). CPKelco A Huber Company www.cpkelco.com.

Klemm, D., Heublein, B., Fink, H. P., & Bohn, A. (2005). Cellulose: Fascinating biopolymer and sustainable raw material. *Angewandte Chemie International Edition in English, 44*(22), 3358–3393. https://doi.org/10.1002/anie.200460587

Kool, M. M., Gruppen, H., Sworn, G., & Schols, H. A. (2013). Comparison of xanthans by the relative abundance of its six constituent repeating units. *Carbohydrate Polymers, 98*(1), 914–921. https://doi.org/10.1016/j.carbpol.2013.07.003

Kool, M. M., Gruppen, H., Sworn, G., & Schols, H. A. (2014). The influence of the six constituent xanthan repeating units on the order–disorder transition of xanthan. *Carbohydrate Polymers, 104*, 94–100. https://doi.org/10.1016/j.carbpol.2013.12.073

Krstonošić, V., Milanović, M., & Dokić, L. (2019). Application of different techniques in the determination of xanthan gum-SDS and xanthan gum-Tween 80 interaction. *Food Hydrocolloids, 87*, 108–118. https://doi.org/10.1016/j.foodhyd.2018.07.040

Kumar, A., Rao, K. M., & Han, S. S. (2018). Application of xanthan gum as polysaccharide in tissue engineering: A review. *Carbohydrate Polymers, 180*, 128–144. https://doi.org/10.1016/j.carbpol.2017.10.009

Liu, W., Sato, T., Norisuye, T., & Fujita, H. (1987). Thermally induced conformational change of xanthan in 0.01m aqueous sodium chloride. *Carbohydrate Research, 160*, 267–281. https://doi.org/10.1016/0008-6215(87)80317-8

Lopes, L., Andrade, C. T., Milas, M., & Rinaudo, M. (1992). Role of conformation and acetylation of xanthan on xanthan-guar interaction. *Carbohydrate Polymers, 17*(2), 121–126. https://doi.org/10.1016/0144-8617(92)90105-y

Maarel, J. R. C. (2008). *Introduction to biopolymer physics. Hackensack*. N.J.: World Scientific.

Margaritis, A., & Zajic, J. E. (1978). Mixing, mass transfer, and scale-up of polysaccharide fermentations. *Biotechnology and Bioengineering, 20*(7), 939–1001. https://doi.org/10.1002/bit.260200702

Masuelli, M. A. (2011). Viscometric study of pectin. Effect of temperature on the hydrodynamic properties. *International Journal of Biological Macromolecules, 48*(2), 286–291. https://doi.org/10.1016/j.ijbiomac.2010.11.014

Matsuda, Y., Biyajima, Y., & Sato, T. (2009). Thermal denaturation, renaturation, and aggregation of a double-helical polysaccharide xanthan in aqueous solution. *Polymer Journal, 41*(7), 526–532. https://doi.org/10.1295/polymj.PJ2008300

Melton, L. D., Mindt, L., Rees, D. A., & Sanderson, G. R. (1976). Covalent structure of the extracellular polysaccharide from xanthomonas campestris: Evidence from partial hydrolysis studies. *Carbohydrate Research, 46*(2), 245–257. https://doi.org/10.1016/s0008-6215(00)84296-2

Mendonça, A., Morais, P. V., Pires, A. C., Chung, A. P., & Oliveira, P. V. (2020). A review on the importance of microbial biopolymers such as xanthan gum to improve soil properties. *Applied Sciences, 11*(1). https://doi.org/10.3390/app11010170

Merino-Gonzalez, A., & Kozina, A. (2017). Influence of aggregation on characterization of dilute xanthan solutions. *International Journal of Biological Macromolecules, 105*(Pt 1), 834–842. https://doi.org/10.1016/j.ijbiomac.2017.07.110

Michel, M., Marguerite, R., Robert, D., Redouane, B., & Peter, L. (2002). Small angle neutron scattering from polyelectrolyte solutions: From disordered to ordered xanthan chain conformation. *Macromolecules, 28*(9), 3119–3124. https://doi.org/10.1021/ma00113a014

Milas, M., Reed, W. F., & Printz, S. (1996). Conformations and flexibility of native and re-natured xanthan in aqueous solutions. *International Journal of Biological Macromolecules, 18*(3), 211–221. https://doi.org/10.1016/0141-8130(95)01080-7

Milas, M., & Rinaudo, M. (1979). Conformational investigation on the bacterial polysaccharide xanthan. *Carbohydrate Research, 76*(NOV), 189–196. https://doi.org/10.1016/0008-6215(79)80017-8

Milas, M., & Rinaudo, M. (1986). Properties of xanthan gum in aqueous solutions: Role of the conformational transition. *Carbohydrate Research, 158*(C), 191–204. https://doi.org/10.1016/0008-6215(86)84017-4

Miranda, A. L., Costa, S. S., Assis, D.d. J., Jesus, C. S., Guimarães, A. G., & Druzian, J. I. (2019). Influence of strain and fermentation time on the production, composition, and properties of xanthan gum. *Journal of Applied Polymer Science, 137*(15), Article 48557. https://doi.org/10.1002/app.48557

Morris, E. R. (2019). Ordered conformation of xanthan in solutions and "weak gels": Single helix, double helix - or both? *Food Hydrocolloids, 86*, 18–25. https://doi.org/10.1016/j.foodhyd.2017.11.036

Morris, E. R., & Foster, T. J. (1994). Role of conformation in synergistic interactions of xanthan. *Carbohydrate Polymers, 23*(2), 133–135. https://doi.org/10.1016/0144-8617(94)90038-8

Morris, E. R., Rees, D. A., Young, G., Walkinshaw, M. D., & Darke, A. (1977). Order-disorder transition for a bacterial polysaccharide in solution. A role for polysaccharide conformation in recognition between Xanthomonas pathogen and its plant host. *Journal of Molecular Biology, 110*(1), 1–16. https://doi.org/10.1016/S0022-2836(77)80095-8

de Moura, M. R. V., & Moreno, R. B. Z. L. (2019). Concentration, brine salinity and temperature effects on xanthan gum solutions rheology. *Applied Rheology, 29*(1), 69–79. https://doi.org/10.1515/arh-2019-0007

Norton, I. T., Goodall, D. M., Frangou, S. A., Morris, E. R., & Rees, D. A. (1984). Mechanism and dynamics of conformational ordering in xanthan polysaccharide. *Journal of Molecular Biology, 175*(3), 371–394. https://doi.org/10.1016/0022-2836(84)90354-1

Nsengiyumva, E. M., & Alexandridis, P. (2022). Xanthan gum in aqueous solutions: Fundamentals and applications. *International Journal of Biological Macromolecules, 216*, 583–604. https://doi.org/10.1016/j.ijbiomac.2022.06.189

Orentas, D. G., Sloneker, J. H., & Jeanes, A. (1963). Pyruvic acid content and constituent sugars of exocellular polysaccharides from different species of genus xanthomonas. *Canadian Journal of Microbiology, 9*(3), 427. https://doi.org/10.1139/m63-055

Oviatt, H. W., & Brant, D. A. (2002). Viscoelastic behavior of thermally treated aqueous xanthan solutions in the semidilute concentration regime. *Macromolecules, 27*(9), 2402–2408. https://doi.org/10.1021/ma00087a007

Pelletier, E., Viebke, C., Meadows, J., & Williams, P. A. (2001). A rheological study of the order-disorder conformational transition of xanthan gum. *Biopolymers, 59*(5), 339–346. https://doi.org/10.1002/1097-0282(20011015)59:5<339::AID-BIP1031>3.0.CO;2-A

Petri, D. F. S. (2015). Xanthan gum: A versatile biopolymer for biomedical and technological applications. *Journal of Applied Polymer Science, 132*(23), 42035–42048. https://doi.org/10.1002/app.42035

Rinaudo, M., Milas, M., Bresolin, T., & Ganter, J. (1999). Physical properties of xanthan, galactomannan and their mixtures in aqueous solutions. *Macromolecular Symposia, 140*(1), 115–124. https://doi.org/10.1002/masy.19991400113

Rochefort, W. E., & Middleman, S. (1987). Rheology of xanthan gum: Salt, temperature, and strain effects in oscillatory and steady shear experiments. *Journal of Rheology, 31*(4), 337–369. https://doi.org/10.1122/1.549953

Sandford, P. A., & Baird, J. (1983). 7 - industrial utilization of polysaccharides. In G. O. Aspinall (Ed.), *The polysaccharides* (pp. 411–490). Academic Press.

Shatwell, K. P., Sutherland, I. W., Dea, I. C. M., & Ross-Murphy, S. B. (1990). The influence of acetyl and pyruvate substituents on the helix-coil transition behaviour of xanthan. *Carbohydrate Research, 206*(1), 87–103. https://doi.org/10.1016/0008-6215(90)84009-j

Southwick, J. G., Jamieson, A. M., & Blackwell, J. (1982). Conformation of xanthan dissolved in aqueous urea and sodium chloride solutions. *Carbohydrate Research, 99*(2), 117–127. https://doi.org/10.1016/s0008-6215(00)81902-3

Tako, M., Teruya, T., Tamaki, Y., & Ohkawa, K. (2010). Co-gelation mechanism of xanthan and galactomannan. *Colloid and Polymer Science, 288*(10–11), 1161–1166. https://doi.org/10.1007/s00396-010-2242-6

Tomofuji, Y., Matsuo, K., & Terao, K. (2022). Kinetics of denaturation and renaturation processes of double-stranded helical polysaccharide, xanthan in aqueous sodium chloride. *Carbohydrate Polymers, 275*, Article 118681. https://doi.org/10.1016/j.carbopol.2021.118681

Viebke, C. (2005). Chapter 17. Order-Disorder conformational transition of xanthan gum. In *ChemInform, 37* pp. 459–474). Weinheim: WILEY-VCH Verlag.

Wang, S., He, L., Guo, J., Zhao, J., & Tang, H. (2015). Intrinsic viscosity and rheological properties of natural and substituted guar gums in seawater. *International Journal of Biological Macromolecules, 76*, 262–268. https://doi.org/10.1016/j.ijbiomac.2015.03.002

Wever, D. A. Z., Picchioni, F., & Broekhuis, A. A. (2011). Polymers for enhanced oil recovery: A paradigm for structure–property relationship in aqueous solution. *Progress in Polymer Science, 36*(11), 1558–1628. https://doi.org/10.1016/j.progpolymsci.2011.05.006

Wyatt, N. B., Gunther, C. M., & Liberatore, M. W. (2011). Increasing viscosity in entangled polyelectrolyte solutions by the addition of salt. *Polymer, 52*(11), 2437–2444. https://doi.org/10.1016/j.polymer.2011.03.053

Wyatt, N. B., & Liberatore, M. W. (2009). Rheology and viscosity scaling of the polyelectrolyte xanthan gum. *Journal of Applied Polymer Science, 114*(6), 4076–4084. https://doi.org/10.1002/app.31093

Wyatt, N. B., & Liberatore, M. W. (2010). The effect of counterion size and valency on the increase in viscosity in polyelectrolyte solutions. *Soft Matter, 6*(14), 3346–3352. https://doi.org/10.1039/c000423e

Xia, S., Zhang, L., Davletshin, A., Li, Z., You, J., & Tan, S. (2020). Application of polysaccharide biopolymer in petroleum recovery. *Polymers, 12*(9). https://doi.org/10.3390/polym12091860

Xu, L., Xu, G., Liu, T., Chen, Y., & Gong, H. (2013). The comparison of rheological properties of aqueous welan gum and xanthan gum solutions. *Carbohydrate Polymers, 92*(1), 516–522. https://doi.org/10.1016/j.carbpol.2012.09.082

Yu, Y., Shen, M., Song, Q., & Xie, J. (2018). Biological activities and pharmaceutical applications of polysaccharide from natural resources: A review. *Carbohydrate Polymers, 183*, 91–101. https://doi.org/10.1016/j.carbpol.2017.12.009

Zhang, L. M., Zhou, J. F., & Hui, P. S. (2005). A comparative study on viscosity behavior of water-soluble chemically modified guar gum derivatives with different functional lateral groups. *Journal of the Science of Food and Agriculture, 85*(15), 2638–2644. https://doi.org/10.1002/jsfa.2308